CHEMISTRY
A EUROPEAN JOURNAL

DOI: 10.1002/chem.201002878

Structural Design, Solid-Phase Synthesis and Activity of Membrane-Anchored β-Secretase Inhibitors on Aβ Generation from Wild-Type and Swedish-Mutant APP

Heinke Schieb,[c] Sebastian Weidlich,[a] Georg Schlechtingen,[a, b] Philipp Linning,[a] Gary Jennings,[b] Margit Gruner,[a] Jens Wiltfang,[c] Hans-Wolfgang Klafki,*[c] and Hans-Joachim Knölker*[a, b]

Abstract: Covalent coupling of β-secretase inhibitors to a raftophilic lipid anchor via a suitable spacer by using solid-phase peptide synthesis leads to tripartite structures displaying substantially improved inhibition of cellular secretion of the β-amyloid peptide (Aβ). Herein, we describe a series of novel tripartite structures, their full characterization by NMR spectroscopy and mass spectrometry, and the analysis of their biological activity in cell-based assays. The tripartite structure concept is applicable to different pharmacophores, and the potency in terms of β-secretase inhibition can be optimized by adjusting the spacer length to achieve an optimal distance of the inhibitor from the lipid bilayer. A tripartite structure containing a transition-state mimic inhibitor was found to be less potent on Aβ generation from Swedish-mutant amyloid precursor protein (APP) than from the wild-type protein. Moreover, our observations suggest that specific variants of Aβ are generated from wild-type APP but not from Swedish-mutant APP and are resistant to β-secretase inhibition. Efficient inhibition of Aβ secretion by tripartite structures in the absence of appreciable neurotoxicity was confirmed in a primary neuronal cell culture, thus further supporting the concept.

Keywords: Alzheimer's disease · lipid rafts · membranes · peptide synthesis · beta-secretase inhibition

Introduction

The membrane-bound enzyme β-secretase plays a key role in the processing of the amyloid precursor protein (APP) to generate amyloid β (Aβ)-peptides, the major protein components of plaques in Alzheimer's disease.[1] The transmembrane protein β-*site APP cleaving enzyme 1* (BACE1) was discovered to have the predominant β-secretase activity in human brain.[2] BACE1 and APP are co-localized in the membrane, where BACE1 cleaves off the soluble, N-terminal fragment sAPPβ. Subsequent cleavage of the remaining 99 amino acid C-terminal APP fragment by the γ-secretase complex produces Aβ-peptides. β-Secretase inhibitors are of interest as potential therapeutics for Alzheimer's disease.[3]

BACE1 has been located at the Golgi network, in endosomes and at the cell surface.[4] BACE1 is transported between cell membrane and endosomes by endocytosis. The amyloidogenic cleavage of APP by BACE1 can occur in lipid rafts.[5] Lipid rafts are structural domains of the membrane enriched in cholesterol, sphingolipids, and certain proteins.[6] For efficacy in living cells, BACE inhibitors either have to cross two membranes, or have to be anchored in the outer leaflet of the cell membrane before the endosome is generated by endocytosis. Certain sterols, such as cholesterol and dihydrocholesterol (Dhc-OH), partition selectively into the lipid rafts on their interaction with membranes.[6] We call compounds displaying such affinity "raftophiles". Based on these considerations, we described in 2005 our concept of

[a] Dr. S. Weidlich, Dr. G. Schlechtingen, P. Linning, Dr. M. Gruner, Prof. Dr. H.-J. Knölker
Department of Chemistry
Technische Universität Dresden
Bergstrasse 66, 01069 Dresden (Germany)
Fax: (+49) 351-463-37030
E-mail: hans-joachim.knoelker@tu-dresden.de

[b] Dr. G. Schlechtingen, Dr. G. Jennings, Prof. Dr. H.-J. Knölker
JADO Technologies GmbH
Tatzberg 47–51, 01307 Dresden (Germany)

[c] H. Schieb, Prof. Dr. J. Wiltfang, Dr. H.-W. Klafki
Department of Psychiatry and Psychotherapy
University of Duisburg-Essen
LVR-Klinikum, Essen (Germany)

Supporting information for this article is available on the WWW under http://dx.doi.org/10.1002/chem.201002878.

the "tripartite structures", in which β-secretase inhibitors (or differerent pharmacophores for further applications) are targeted to the lipid rafts by linking them through an appropriate spacer to a membrane anchor (Figure 1).[7]

Figure 1. General principle of the tripartite structures consisting of membrane anchor (raftophile), spacer and pharmacophore (inhibitor).

Rapid cellular internalization, accumulation in endosomes, and raft partitioning of a prototype tripartite peptidic transition state β-secretase inhibitor has been subsequently demonstrated by us.[8] Furthermore, the tripartite structure was shown to efficiently inhibit Aβ production in transfected cells and in vivo in transgenic mice. Importantly, the potency of the membrane targeted inhibitor was markedly improved as compared to the free inhibitor, providing a compelling "proof of principle" for our tripartite concept.[8]

In the present study, we describe in detail the solid-phase synthesis of a series of tripartite structure compounds, their full characterization by NMR spectroscopy, and the analysis of their biological activity in cell-based assays. As a continuation of our previous work using the original peptidic prototype tripartite BACE inhibitor,[8] the present detailed study provides answers to the following fundamental questions:

1. Is the tripartite structure concept applicable to a different, non-peptidic small molecule pharmacophore?
2. Is there an optimal spacer length for highly efficient BACE inhibition?
3. Do the compounds work equally well in primary neuronal cells without causing neurotoxicity?
4. Are tripartite inhibitors equally efficient on the Aβ generation from wild-type APP and from APP carrying the Swedish double mutation (KM-NL 670/671), which is known to increase the BACE-dependent Aβ production considerably?[9]
5. Are the concentrations of different N- or C-terminal variants of Aβ reduced to the same extent by a tripartite structure BACE-inhibitor?

Results and Discussion

Two known inhibitors have been used for this study: The commercial transition state mimic **1** (GL 189 from Calbiochem/Merck), which completely inhibits BACE in vitro at 5 μM in assays based on solubilized membrane fractions,[3b,10,11] and the lysine derivative **2** (Elan Pharmaceuticals/Pharmacia & Upjohn).[12]

Dihydrocholesterol has been used as membrane anchor and has been introduced by esterification of 9-fluorenylmethoxycarbonyl(Fmoc)-protected *tert*-butyl aspar-

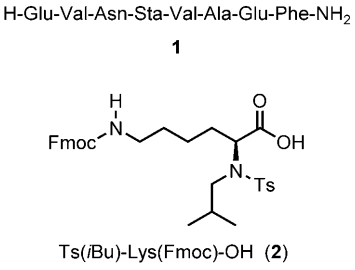

Ts(*i*Bu)-Lys(Fmoc)-OH (**2**)

tate **3** using 1-(2-mesitylenesulfonyl)-3-nitro-1*H*-1,2,4-triazole (MSNT) (Scheme 1).[13] Subsequent cleavage of the *tert*-butyl ester **3a** afforded **4**. The Fmoc-protected aspartate

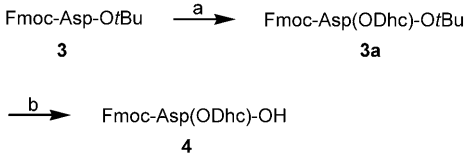

Scheme 1. Synthesis of the membrane-anchor building block **4**. Reagents and conditions: a) MSNT, *N*-methylimidazole, dihydrocholesterol, CH_2Cl_2, RT, 4 h (84%), (Dhc = Dihydrocholesten-3-yl); b) CF_3COOH, CH_2Cl_2, RT, 75 min (85%).

with dihydrocholesterol in its side chain represents a building block useful for solid-phase peptide synthesis.

To reach the active site of the enzyme, the inhibitor must be present at a certain distance from the membrane. Thus, linkage of the raftophile building block **4** and inhibitor **1** has been achieved by using the amino(oligoethyleneglycol)carboxylic acids H-3Gl-OH and H-4Gl-OH as spacer fragments, which are commercially available as their *N*-Fmoc derivatives **5** and **6** (Scheme 2; H-3Gl-OH: 12-amino-4,7,10-

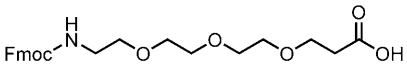

Fmoc-3Gl-OH (**5**)

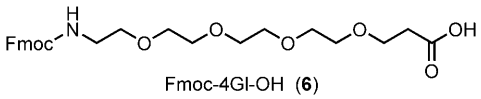

Fmoc-4Gl-OH (**6**)

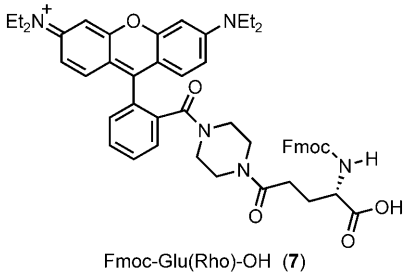

Fmoc-Glu(Rho)-OH (**7**)

Scheme 2. Spacer building blocks: Fmoc-protected amino(oligoethyleneglycol)carboxylic acids Fmoc-3Gl-OH (**5**) and Fmoc-4Gl-OH (**6**) and fluorophore label: Fmoc-Glu(Rho)-OH (**7**).

Table 1. Structures and molecular masses (as confirmed by ESI-MS) of the tripartite compounds **8a–8i** and **9** prepared by solid-phase peptide synthesis.

No.	Structure	Formula	M [g mol^{-1}]	Spacer length [Å]
8a	H-Glu-Val-Asn-Sta-Val-Ala-Glu-Phe-Asp(ODhc)-NH_2	$C_{75}H_{121}N_{11}O_{17}$	1448.8	0
8b	H-Glu-Val-Asn-Sta-Val-Ala-Glu-Phe-4Gl-Asp(ODhc)-NH_2	$C_{86}H_{142}N_{12}O_{22}$	1696.1	18
8c	H-Glu-Val-Asn-Sta-Val-Ala-Glu-Phe-3Gl-4Gl-Asp(ODhc)-NH_2	$C_{95}H_{159}N_{13}O_{26}$	1899.4	35
8d	H-Glu-Val-Asn-Sta-Val-Ala-Glu-Phe-3Gl-3Gl-3Gl-Asp(ODhc)-NH_2	$C_{102}H_{172}N_{14}O_{29}$	2058.5	47
8e	H-Glu-Val-Asn-Sta-Val-Ala-Glu-Phe-4Gl-3Gl-4Gl-Asp(ODhc)-NH_2	$C_{106}H_{180}N_{14}O_{31}$	2146.6	53
8f	H-Glu-Val-Asn-Sta-Val-Ala-Glu-Phe-3Gl-3Gl-3Gl-3Gl-Asp(ODhc)-NH_2	$C_{111}H_{189}N_{15}O_{33}$	2261.8	63
8g	H-Glu-Val-Asn-Sta-Val-Ala-Glu-Phe-4Gl-3Gl-4Gl-3Gl-4Gl-Asp(ODhc)-NH_2	$C_{126}H_{218}N_{16}O_{40}$	2597.2	89
8g′	H-Glu(Rho)-βAla-Gly-Glu-Val-Asn-Sta-Val-Ala-Glu-Phe-4Gl-3Gl-4Gl-3Gl-4Gl-Asp(ODhc)-NH_2	$C_{168}H_{270}N_{23}O_{46}^+$	3348.1	89
8h	H-Glu-Val-Asn-Sta-Val-Ala-Glu-Phe-4Gl-3Gl-4Gl-3Gl-4Gl-3Gl-4Gl-Asp(ODhc)-NH_2	$C_{146}H_{256}N_{18}O_{49}$	3047.7	123
8i	H-Glu-Val-Asn-Sta-Val-Ala-Glu-Phe-4Gl-3Gl-4Gl-3Gl-4Gl-NH_2	$C_{95}H_{167}N_{15}O_{37}$	2111.4	89
9	Ts(*i*Bu)-Lys(Fmoc)-3Gl-3Gl-3Gl-Asp(ODhc)-NH_2	$C_{90}H_{141}N_7O_{20}S$	1673.2	47

trioxadodecanoic acid; H-4Gl-OH: 15-amino-4,7,10,13-tetraoxapentadecanoic acid). These compounds represent perfect building blocks for the spacer because they have low toxicity, are stable to biodegradation, provide high solubility, and enable the construction of spacers with defined length by peptide coupling.

To detect the membrane-anchored inhibitors in biophysical assays, fluorophore-labeled derivatives of our tripartite structures have been prepared (see below). Coupling of rhodamine B piperazide[14] to Fmoc-Glu-O*t*Bu followed by ester cleavage with trifluoroacetic acid (TFA) provided Fmoc-Glu(Rho)-OH (**7**) (Scheme 2).

From these building blocks our tripartite structures **8** could be prepared using solid-phase peptide synthesis (PAL-PEG-PS resin (PAL: peptide amide linker; PEG: polyethylene glycol; PS: polystyrene), 1-[bis(dimethylamino)methylene]-1*H*-1,2,3-triazolo[4,5-*b*]pyridinium 3-oxide hexafluorophosphate (HATU) and 1-[bis(dimethylamino)methylene]-1*H*-benzotriazolium 3-oxide hexafluorophosphate (HBTU) activation)[15] (see Experimental Section and Table 1). The peptides **8a–i** and **9** were purified by preparative HPLC and characterized by mass spectrometry. For peptide **8e**, a full assignment of the ^{1}H and ^{13}C NMR spectra has been achieved by 2D-NMR spectroscopy (COSY, HMBC, HSQC, ROESY) (Figure 2; see also the Supporting Information). The NMR spectrum confirmed that compound **8e** was obtained as a single diastereoisomer, which emphasized that pure compounds have been applied to the bioassays (purity according to HPLC analysis: >99.9%). The spacer should place the inhibitor in an appropriate distance above the membrane surface to represent an optimal mimic of the APP cleavage site, which thus shows efficient complex formation with the protease domain of β-secretase.[16,17] Diverse combinations of the spacer building blocks **5** and **6** led to a series of tripartite compounds **8a–8h** with the inhibitor **1** as pharmacophore and spacer lengths ranging from 0 to 123 Å. For example, the sequence -4Gl-3Gl-4Gl-3Gl-4Gl- in **8g** provides a spacer of a maximum length of about 89 Å (assuming an all-trans conformation) by just five peptide couplings. Fluorophore-labeled derivatives of the peptides **8** could also be prepared (see the Experimental Section). The rhodamine label **7** can conveniently be attached to the N-terminus through a short linker (βAla-Gly) as executed for compound **8g** providing **8g′**. The β-alanine provides enhanced flexibility and is expected to prevent adoption of unwanted secondary structures. The H-Glu(Rho) fragment is stable during peptide cleavage and deprotection, and therefore, is applied to label the N-terminus of the peptide chain. Biophysical studies using peptide **8g′** confirmed the preferential partitioning of the membrane-anchored inhibitors into the raft phase.[8a,18] Inhibitor **2** was used for the synthesis of tripartite compound **9**, containing a spacer of medium length (47 Å).

For testing the biological activity of the tripartite structures, we have chosen primary chicken telencephalic neuronal cultures (CTN) and SH-SY5Y cell lines expressing either tagged human APP695 wild-type (APPwt: wild-type amyloid precursor protein) or tagged human APP695 carrying the Swedish double mutation KM-NL(670/671) (APPsw: Swedish-mutant amyloid precursor protein). The avian APP sequence has a high homology to human APP, and the C-terminal 104 amino acids including the complete Aβ-peptide region are even identical. Furthermore, the chicken embryo also expresses all enzymes required for Aβ generation including BACE1 and BACE2.[19] As the primary CTN are not genetically modified and are of neuronal origin they reflect physiological brain functions to a greater degree than immortalized cell lines. The transfected SH-SY5Y cell lines are suitable for comparing Aβ generation from wild-type and Swedish-mutant human APP, and they allow a larger number of individual measurements required for calculating reasonable dose-response curves and half-maximal effects (EC_{50} values).

The inhibitor **1** (GL 189), the small-molecule inhibitor **2**, and their corresponding membrane-targeted tripartite structures with 47 Å spacers (**8d** and **9**) were tested at a concentration of 100 nM in all three cell culture models. While the tripartite structures **8d** and **9** efficiently reduced the secretion of Aβ40 in all models, the free inhibitors **1** and **2** had no effect (Figure 3A). No significant decrease of formation of Aβ40 was observed for compounds **1** and **2** at concentrations of up to 10 μM in all three cell models (data not shown). In CTN, compound **9** appeared to be less potent than in SH-SY5Y cells, and increasing the concentration to

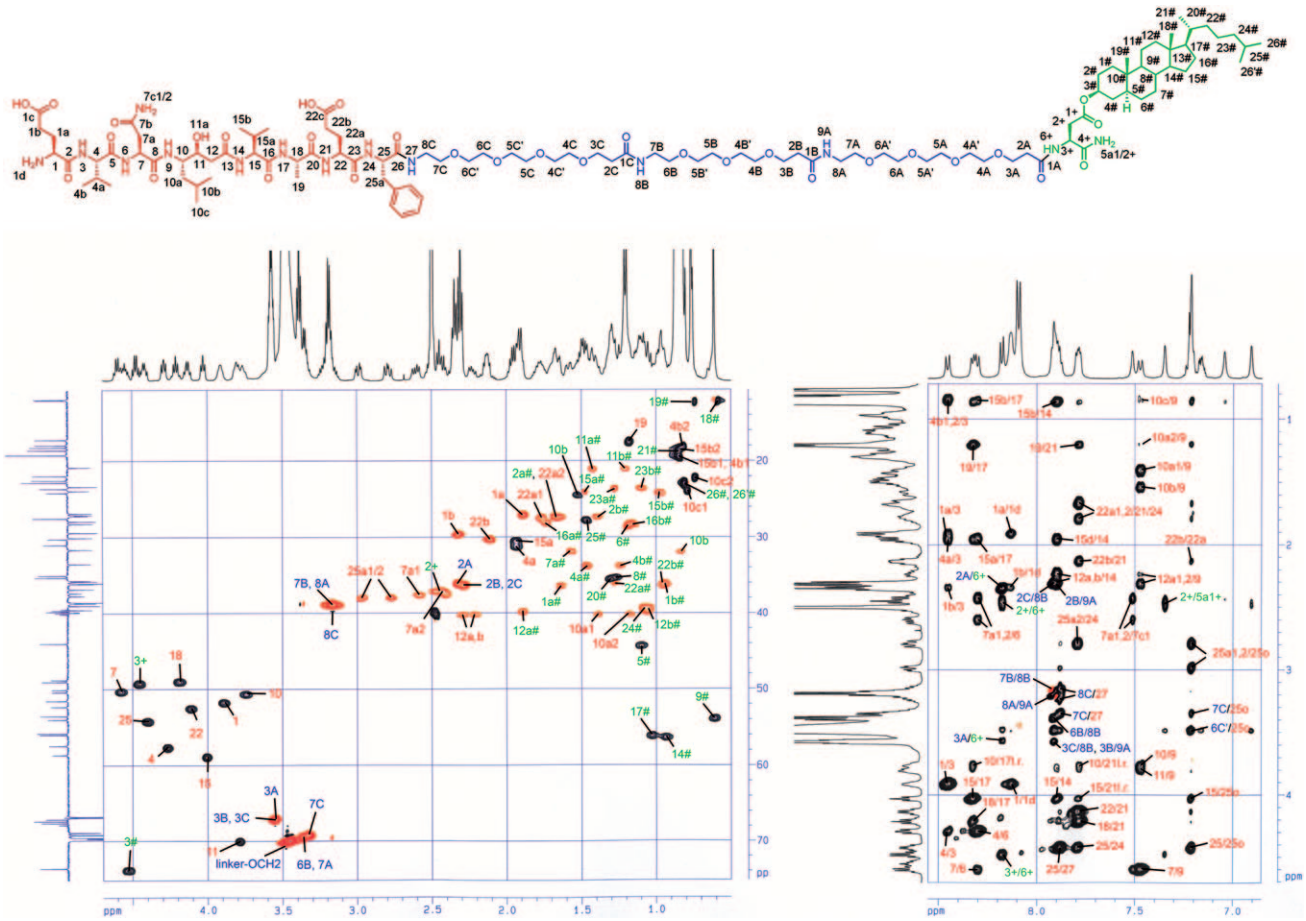

Figure 2. HSQC and ROESY spectra (500 MHz, [D_6]DMSO) of the peptide **8e** with complete assignments of the signals.

1 μM indicated a dose-dependent inhibition of Aβ40 production (Figure 3A). Our findings confirm that membrane targeting can substantially improve the potency of a BACE inhibitor and indicate that the tripartite concept is also applicable to a non-peptidic small-molecule inhibitor. For analysis of the CTN cell culture supernatants, we employed a multiplex assay that simultaneously detects the major Aβ variants Aβ38, Aβ40, and Aβ42. As the β-secretase cleavage of APP generates the N-terminus of Aβ, a specific inhibitor of BACE should not influence the proportions of the different C-terminal variants of Aβ-peptides. As expected, the concentrations of all three different Aβ-peptides were reduced to a similar extent by treating the cells with compounds **8d** or **9** (Figure 3B).

In agreement with the proposed mechanism of action, being the direct inhibition of the β-secretase activity, we observed a significant decrease in secreted sAPPβ from CTN and SH-SY5Y APPwt (the assay does not detect sAPPβsw). This was accompanied by elevated sAPPα suggesting a compensatory increase in α-secretase cleavage (Figure 3C). The increase in sAPPα secretion was confirmed in all three cell types by Western blot analysis (Figure 3D). The amounts of the membrane-bound 99 amino acid C-terminal APP fragment (β-CTF) resulting from β-secretase cleavage were analyzed in lysates from SH-SY5Y cells. As shown in Figure 3D, both tripartite structures **8d** and **9** diminished the cellular C99 β-CTFs, further supporting BACE cleavage to be targeted by the compounds.

To test for possible toxic effects of the tripartite structures under investigation, we employed two different cellular viability assays. The MTT assay monitors mitochondrial functionality, the lactate dehydrogenase (LDH) assay membrane integrity. The absorbance data for CTN cells treated with compound **8d** or **9** are presented in Figure 4 as percentage of controls. Statistically significant differences in the mean absorptions between treated cells and controls (indicating cytotoxicity) were not apparent in either assay with concentrations below 10 μM for compound **8d** and below 100 μM for compound **9**.

To determine the optimal positioning of the inhibitor relative to the membrane, tripartite structures with spacer lengths varying from 18 Å to 123 Å were synthesized. To gain an initial insight into suitable spacer lengths, the structures **8a** to **8i**, as well as the free β-secretase inhibitor **1** were tested at a fixed concentration of 100 nM for their ability to reduce Aβ-peptide secretion. A reduction of about 75–90% of the secretion of Aβ-peptides was achieved with spacer lengths ranging from 35 to 89 Å (Figure 5). The free

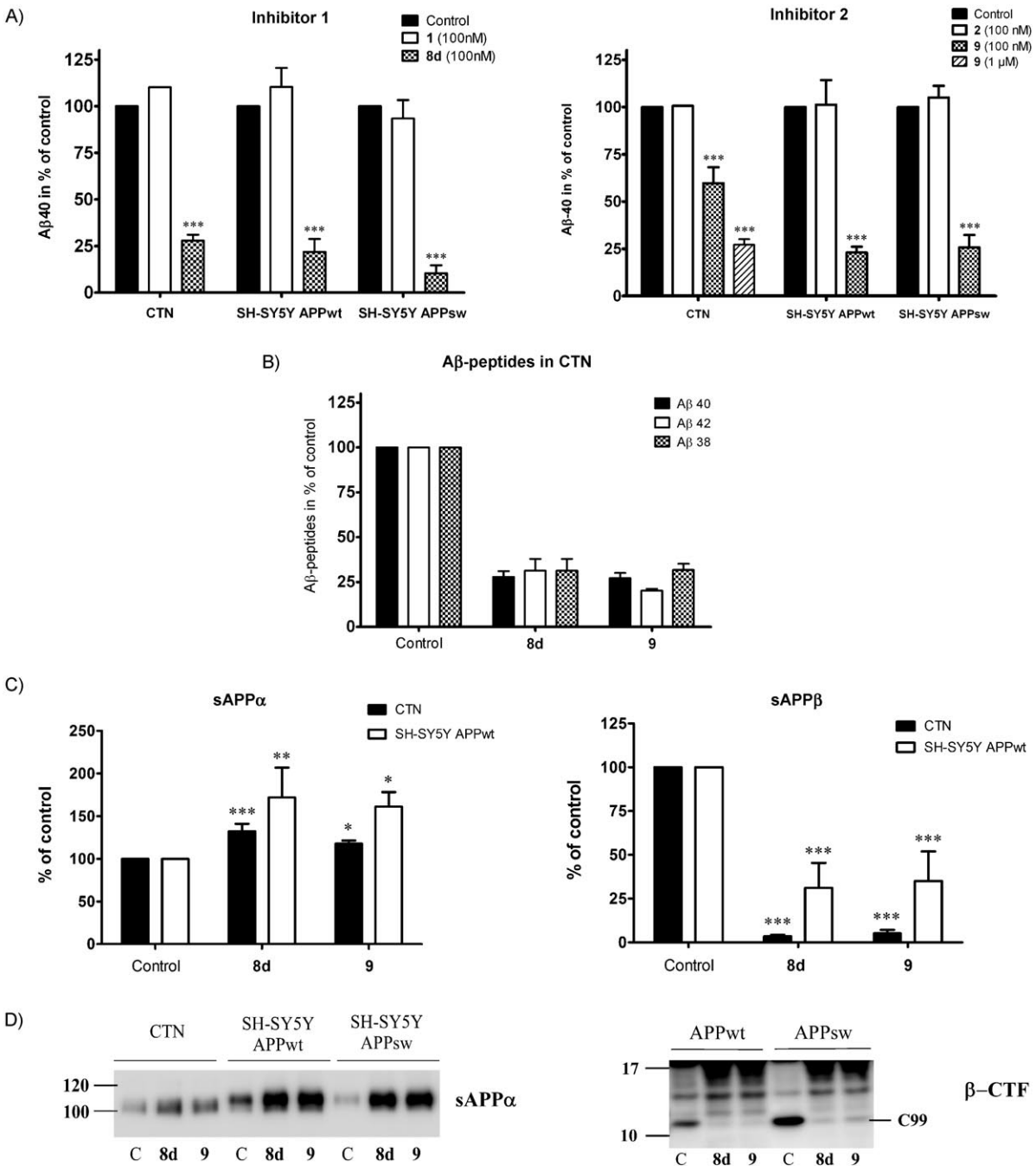

Figure 3. Tripartite structures reduce Aβ-peptides in cellular assays by inhibition of β-secretase cleavage. A) Cells were treated for 20 h (CTN) or 4 h (SH-SY5Y cells) with test compounds, and the supernatants were analyzed with Aβ-ECL assays (Aβ40 assay for SH-SY5Y cells or Aβ-triplex assay for CTN). In CTN, compounds **1** and **2** were tested in one experiment only, all other tests were repeated at least three times (mean ±SD are shown). Aβ40 secretion is expressed in % of the 1% DMSO control. B) The concentrations of Aβ38, Aβ40 and Aβ42 in the supernatants from CTN were reduced in parallel after 20 h treatment with 100 nM of compound **8d** or 1 μM of compound **9**. C) Cell culture supernatants of CTN and SH-SY5Y APPwt cells treated with 100 nM of compound **8d** or **9** were analyzed with the ECL sAPPα/β assay. The amounts of sAPPα and sAPPβ are shown in percent of the control. The increase in sAPPα as well as the decrease in sAPPβ were statistically significant (one-way ANOVA followed by Tukey's post test; *: $p<0.05$; **: $p<0.01$; ***: $p<0.001$). D) After treatment with compounds **8d** and **9** (100 nM and 1 μM, respectively) for 20 h, cell supernatants were collected and the cells were lysed with Triton X-100 lysis buffer. Proteins of the supernatants and lysates were separated by SDS-PAGE and analyzed by Western blot. Secreted sAPPα and β-CTF in cell lysates were detected with the monoclonal antibody 1E8.

inhibitor **1**, the 18 Å-spacer-compound **8b**, and compound **8i** without the membrane anchor were essentially inactive.

The apparent small effect and the relative large variation observed with the 0 Å spacer length presumably derive from the lower solubility of this compound. Compound **8h** with a 123 Å spacer was less efficient than the compounds with spacers ranging from 35 to 89 Å. For an in-depth determination of the optimal spacer length, four selected compounds

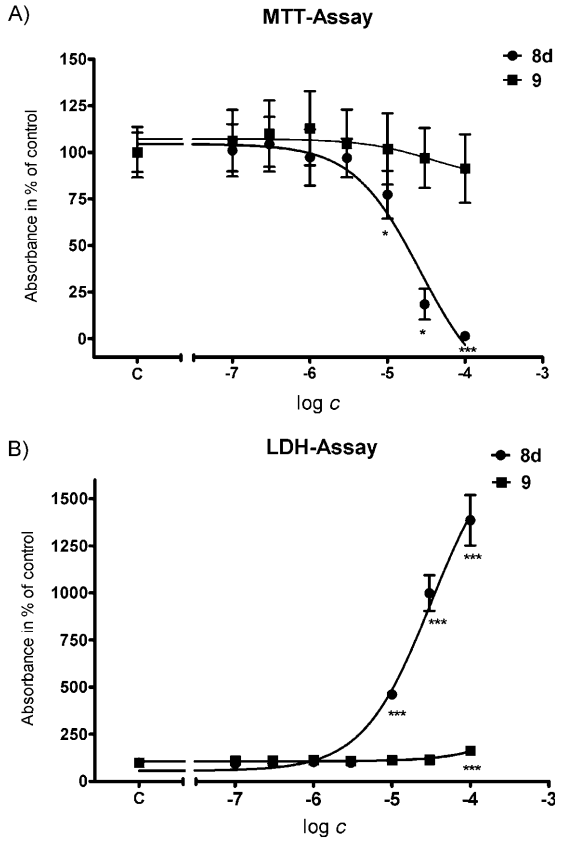

Figure 4. MTT and LDH cell viability assays for compounds **8d** and **9** in CTN. In the MTT assay (A), toxic effects are indicated by a decrease of the absorbance at 550 nm. In the LDH assays (B), release of LDH as a consequence of impaired membrane integrity is indicated by an increase of the absorbance at 490 nm. The data for compounds **8d** and **9** are shown in percent of the controls (mean values ±SD, $n=6$). For statistical analysis, the absorption data for each tested concentration were compared with the control by one-way ANOVA followed by Dunnett's Multiple Comparison test. *$=p<0.05$; ***$=p<0.001$.

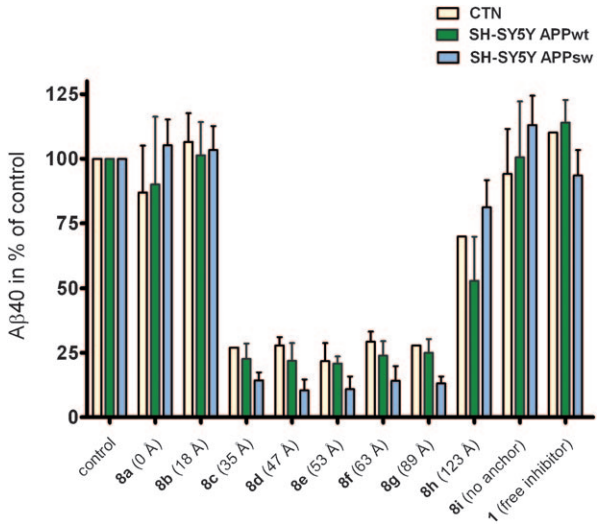

Figure 5. Influence of the spacer lengths of the tripartite structures on inhibition of Aβ40 secretion. Test compounds were added to the culture media at a concentration of 100 nM for 20 h (CTN, 5th day in vitro) or 4 h (SH-SY5Y). Aβ-peptides in the supernatants were measured in duplicates with Aβ40 ECL assays and are shown in percent of the control. For compounds **8a**–**8h** the spacer lengths are given in brackets. In CTN cells compounds **8c**, **8g**, **8h**, and **1** were tested in one experiment only. All other listed compounds were tested at least three times (mean values and the SDs are shown). Note that the results with the compounds **8d** and **1** are the same as shown in Figure 3A and are presented here again for comparison.

(**8c**, **8d**, **8f** and **8g** in Table 1) with spacers ranging from 35 to 89 Å were tested in serial dilutions with SH-SY5Y APPwt and SH-SY5Y APPsw cells. The amount of Aβ40 secreted from the treated cells was normalized to percent of the DMSO controls, and the results from three independent experiments were combined to calculate dose-response curves and the concentrations resulting in EC_{50} values by nonlinear regression (Figure 6). The null hypothesis (i.e. all calculated logEC_{50} values are the same) could be rejected by extra sum-of-squares F test ($p<0.0001$ for APPwt and $p<0.001$ for APPsw).

In both cell lines, the lowest EC_{50} values (i.e. the highest potencies) were observed with compound **8g** (89 Å spacer length) (Figure 6 and Table 2). Interestingly, for both APPwt and APPsw the rank order of potencies for the four tested spacer lengths was not linear: the compound with 47 Å spacer length showed the second-best potency, whereas the compounds with 35 Å and 63 Å spacer lengths were less efficient. This was observed in each individual experiment ($n=3$) per se, as well as in the combined data analysis shown in Figure 6 and Table 2. Compounds **8c** and **8f** with 35 Å and 63 Å linkers displayed comparable potencies. Our findings suggest that the β-secretase cleavage of APP tolerates some variation with regard to the distance to the membrane. This is in agreement with findings from an earlier study by Citron and co-workers, in which β-secretase substrate requirements were analyzed with the aid of several APP deletion and amino acid substitution constructs.[20] The EC_{50} values of all four tested tripartite structures that we tested herein were lower in cells expressing APPwt than in cells expressing APPsw. For example: for compound **8g** the EC_{50} values were about 0.4 nM for APPwt and about 5 nM for APPsw (Figure 6C and Table 2). This is consistent with published observations and may reflect "aberrant subcellular location of APPsw processing"[21] or may be related to the finding that APPsw is a better substrate for BACE than APPwt.[22] Under the experimental conditions employed, neither in SH-SY5Y APPwt nor in SH-SY5Y APPsw cells did the tripartite structures completely abolish the secretion of Aβ40 into the cell culture medium. As indicated by the lower plateau of the dose-response curves shown in Figure 6 and Table 2, about 5–10% of the Aβ40 secretion from SH-SY5Y APPsw and about 20–28% from SH-SY5Y APPwt were apparently resistant to the treatment with tripartite structures under these experimental conditions. Following an overnight incubation with the tripartite structures at a concentration of 1 μM, approximately 7% (as compared to controls) of the remaining Aβ40 was measured with SH-SY5Y APPsw cells and approximately 20% with SH-SY5Y

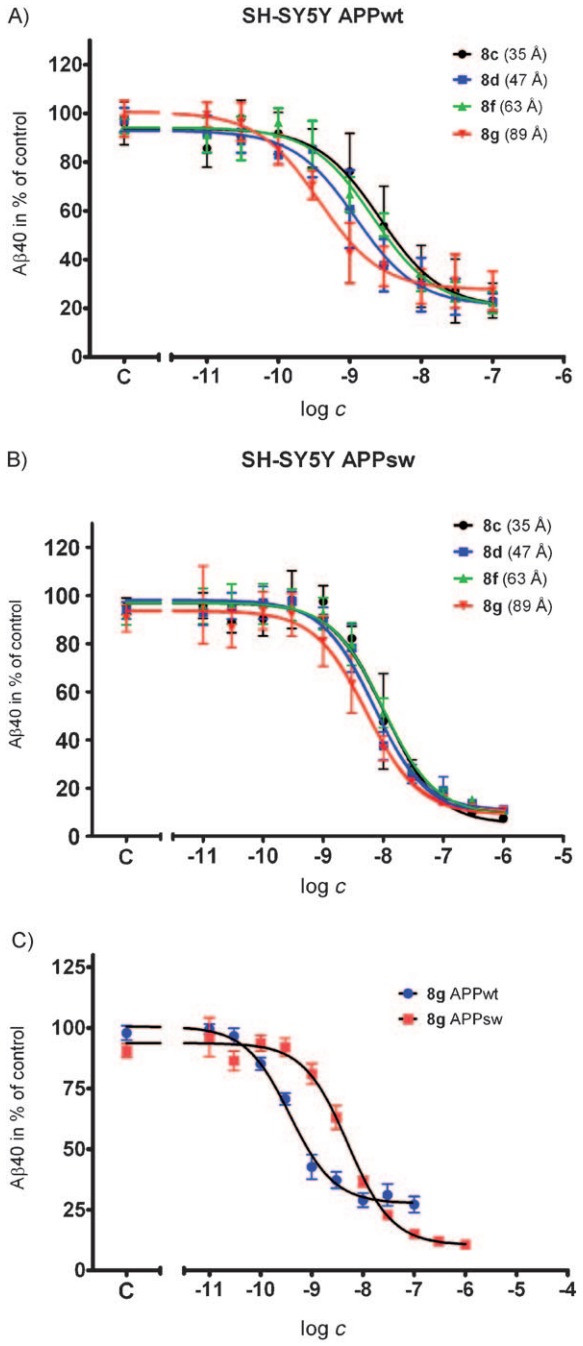

Figure 6. Dose–response curves: Inhibition of Aβ40 secretion by tripartite structures with different spacers. A) Compounds **8c**, **8d**, **8f**, and **8g** were tested at concentrations ranging from 10 pM to 100 nM in SH-SY5Y APPwt cells. Means ±SD of the normalized and pooled data from three independent experiments are shown. C = 1% DMSO as control. B) The same compounds were tested in SH-SY5Y APPsw cells. The dose–response curves were calculated from the normalized and pooled measurements from three independent experiments with two different concentration ranges tested. C) Comparison between dose–response curves for compound **8g** measured in SH-SY5Y APPwt and APPsw.

Table 2. EC_{50} values of tripartite structures with varying spacer lengths on inhibition of Aβ secretion from transfected SH-SY5Y cells.

Compound	Spacer length [Å]	APPwt[a] EC_{50} [nM][b]	APPwt[a] 95% confidence interval EC_{50} [nM]	APPwt[a] lower plateau [%][c]	APPsw[a] EC_{50} [nM][b]	APPsw[a] 95% confidence interval EC_{50} [nM]	APPsw[a] lower plateau [%][c]
8c	35	2.63	1.62–4.29	20.32	10.90	7.76–15.30	5.24
8d	47	1.21	0.89–1.81	21.16	6.80	5.25–8.82	10.64
8f	63	2.11	1.58–2.81	20.54	10.01	7.89–12.7	8.93
8g	89	0.37	0.27–0.52	27.58	5.09	3.73–6.94	10.42

[a] APPwt = Wild-type amyloid precursor protein; APPsw = Swedish-mutant amyloid precursor protein. [b] Half-maximal effect (EC_{50}) of inhibition of Aβ40 secretion from treated cells relative to control (1% DMSO). [c] Lower plateau of the dose–response curve (see Figure 6).

APPwt cells (data not shown). Therefore it seems unlikely that these Aβ-peptides simply reflected the fraction secreted in the period before the inhibitor had reached its site of action. To complement our quantitative Aβ40 measurements with information regarding specific variants of Aβ released from the cells, we employed a novel urea-SDS-PAGE protocol (SDS: sodium dodecyl sulfate; PAGE: polyacrylamide gel electrophoresis), which allows the electrophoretic resolution of several N- and C-terminal Aβ-peptide variants. Western immunoblot detection was achieved with the monoclonal antibody 6E10, which detects several N-terminal variants of Aβ, such as Aβ(1-40), Aβ(2-40), Aβ(3-40), Aβ(4-40), and Aβ(5-40).[23] The same antibody also served as detection antibody in the quantitative electrochemiluminescence (ECL) assays described above. In the cell culture supernatants from SH-SY5Y APPsw cells five different variants of Aβ-peptides were observed, presumably corresponding to Aβ(1-37), Aβ(1-38), Aβ(1-39), Aβ(1-40), and Aβ(1-42).[24] The concentrations of all these Aβ-peptides were substantially reduced in cells treated with 100 nM of the tripartite inhibitors (Figure 7A). In the supernatants from SH-SY5Y cells expressing wild-type APP one additional Aβ-peptide band was regularly detected, which co-migrated with synthetic Aβ(2-40) and also with Aβ(3-40) (both have the same electrophoretic mobility). On treatment with the inhibitors **8g**, **8d**, and **9**, the concentration of this particular Aβ-peptide was apparently not decreased but perhaps even slightly increased (Figure 7A). The free inhibitors **1** and **2** did not influence the Aβ-peptide patterns. To further characterize the additional, BACE inhibitor-resistant Aβ-peptide(s) released from APPwt, we employed two-dimensional (2D) electrophoresis. Owing to the loss of Asp1 the isoelectric point (pI) of N-terminal truncated Aβ-peptides is shifted to a more alkaline pH.[25] 2D SDS-PAGE/Western blot analysis showed that the majority of Aβ-peptides released from SH-SY5Y APPwt cells starts with Asp1 and displays a pI of 5.4. Two faint additional Aβ-spots were observed with a pI of approximately 5.7 and a pI of approximately 6.3, respectively (Figure 7B). In supernatants from cells treated with compound **8g**, the Aβ spots with a pI of approximately 5.4 were drastically diminished, whereas the two more alkaline Aβ forms seemed to be increased. This supports our conclusion that at least one of the Aβ-peptides resistant to BACE inhibition is most probably N-terminal truncated Aβ(2-40) or Aβ(3-40). Consistent with the 1D data, Aβ-peptides with a shifted pI

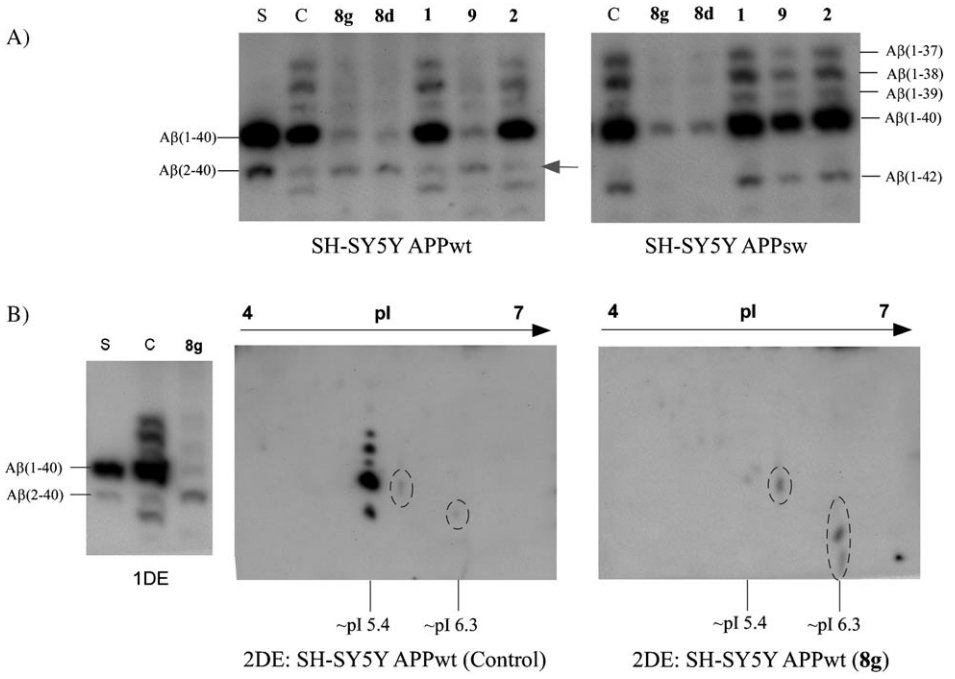

Figure 7. Tripartite structures have different effects on Aβ-peptide secretion from cells expressing APPwt and APPsw. Cells were treated for 20 h with different compounds. Aβ-peptides were immunoprecipitated from the supernatants with the monoclonal antibody 6E10. A) Aβ-peptides were separated by urea-SDS-PAGE, followed by Western blotting and immunostaining with 6E10. A specific Aβ-form comigrating with Aβ(2-40) and generated from APPwt was apparently resistant to inhibition by the compounds **8g**, **8d**, and **9** (arrow). B) Aβ-peptides from SH-SY5Y APPwt cells treated either with 1% DMSO or **8g** were first separated according to their charge on IPG strips with a linear pH range of 4 to 7. Subsequently they were separated according to their charge/mass ratio by Aβ-urea-SDS-PAGE and visualized by immunoblot with 6E10. The presumed N-truncated Aβ spots are encircled. On the left hand side the same samples are shown after a 1D separation. S = Synthetic peptides: Aβ(1-40) (250 pg) and Aβ(2-40) (50 pg) are shown on the left hand side. C = 1% DMSO as control.

value were not observed in SH-SY5Y cells expressing APPsw (data not shown).

This observation provides a possible explanation for the higher proportion of inhibitor-resistant residual Aβ production in APPwt-producing cells. The cellular secretion of Aβ-peptides with N-termini other than Asp1 from APPwt and the possibility of selective pharmacological manipulation has been reported before.[26] The findings were interpreted as evidence for the existence of biochemically distinct β-secretase-type proteases able to create the various N-termini of Aβ-peptides.[26a] Extensive N-terminal heterogeneity of Aβ-peptides in human amyloid plaques from patients with Alzheimer's disease has been reported[27] and may substantially contribute to the physicochemical properties of authentic plaque cores.[28] The most prominent N-truncated Aβ form starts at residue 3 cyclized to pyroglutamate (AβN3pE)[29] and is particularly prone to formation of β-sheets and aggregation.[30] The molecular details as well as the intracellular or extracellular location of the generation of the N-truncated Aβ-peptides and the conversion of glutamate to pyroglutamate have not been fully elucidated.

Conclusion

In conclusion, our observations support the concept of membrane targeting for improved BACE inhibition. By concentrating the inhibitor at the site of action, the required dose is reduced and toxic or other side effects are minimized. We have demonstrated that the principle is applicable to different pharmacophores and that an optimal inhibitory effect can be achieved by adjusting the spacer module according to the molecular properties of APP. Moreover, we report significant differences in terms of Aβ-peptide secretion from wild-type versus Swedish-mutant APP. Since modified Aβ-peptides may be of particular pathophysiological relevance, we believe that the observation of specific Aβ-peptide variants generated from APPwt in spite of the presence of an efficient β-secretase inhibitor is intriguing. Our data support the idea of the existence of more than one enzyme displaying β-secretase activity. The tripartite structure approach provides a highly attractive tool for future studies further addressing the biology of APP and the proposed existence of multiple β-secretases.

Experimental Section

Syntheses

General: The spacer building blocks (Fmoc-3Gl-OH (**5**) and Fmoc-4Gl-OH (**6**)) and statine were purchased from PolyPeptide, France. The other amino acids were purchased from Novabiochem. HATU and Fmoc-PAL-PEG-PS resin were purchased from Applied Biosystems. All reactions were carried out using dry, reagent-grade solvents under argon unless stated otherwise. Flash chromatography was carried out using Merck silica gel (0.040–0.063 mm). Peptide syntheses were executed on an ABI 433A peptide synthesizer equipped with a UV detector. NMR spectra: Bruker DRX 500 and Bruker AC 300; δ in ppm, J in Hz. Mass spectra: Bruker Esquire LC Electrospray MS or MDS Sciex QSTAR Pulsar i quadrupole time-of-flight MS. Isotopic patterns were simulated by using CS ChemDraw 8.0. The most abundant mass is given as theoretical mass.

Analytical HPLC was carried out on an Agilent Model 1100 equipped with a G1315B UV-DAD, a G1321A fluorescence detector and an evaporative light scattering detector (Polymer Laboratories ELS 1000). Column: Vydac 208TP104 (reverse-phase C8, 4.6×250 mm). Flow rate. 1.0 mL min^{-1}. Eluent A: H_2O + 0.1% TFA, eluent B: MeCN + 0.1% TFA. UV detection at 215, 260, and 560 nm. Other conditions (gradient) as stated for the individual compounds.

Preparative HPLC was carried out using a Varian PrepStar system equipped with a Varian ProStar Model 320 UV detector and an evaporative light scattering detector (Polymer Laboratories ELS 1000) connected via an Sunchrom QuickSplit splitter. Column: Vydac 208TP1030 (reverse-phase C8, 30×250 mm). Flow rate: 40 mL min^{-1}. Eluent A: H_2O + 0.1% TFA, eluent B: MeCN + 0.1% TFA. Other conditions (gradient) as stated for the individual compounds.

Synthesis of the membrane-anchor building block 4:

*Fmoc-Asp(ODhc)-OtBu (**3a**)*: Fmoc-Asp-O*t*Bu (**3**) (1.75 g, 4.25 mmol) and MSNT (1.25 g, 4.24 mmol) were suspended in CH_2Cl_2 (12 mL). *N*-Methylimidazole (384 mg, 337 μL, 4.24 mmol) was added and the mixture was stirred for 5 min at room temperature. Dihydrocholesterol (1.5 g, 3.86 mmol) was added. Additional CH_2Cl_2 (7 mL) was added to produce a clear solution. After stirring for 4 h at room temperature, the mixture was partitioned between 2% aqueous citric acid and CH_2Cl_2, washed with 2% citric acid, H_2O, and a saturated solution of $NaHCO_3$. A saturated solution of NH_4Cl was added to separate the phases of the alkaline extraction, and the organic layer was dried over Na_2SO_4. Removal of the solvent and flash chromatography (petroleum ether/Et_2O [3:1] + 1% MeOH) of the residue on silica provided **3a** as a colorless solid (2.80 g; 84%). ^{1}H NMR (300 MHz, $CDCl_3$): δ=0.64 (s, 3H), 1.46 (s, 9H), 0.75–1.90 (m, 42H), 1.95 (br d, J=12.3 Hz, 1H), 2.79 (dd, J=16.8, 4.5 Hz, 1H), 2.95 (dd, J=16.8, 4.5 Hz, 1H), 4.22 (t, J=7.2 Hz, 1H), 4.36 (m, 2H), 4.50 (m, 1H), 4.71 (m, 1H), 5.77 (br d, J=8.4 Hz, 1H), 7.30 (t, J=7.4 Hz, 2H), 7.39 (t, J=7.3 Hz, 2H), 7.59 (d, J=7.3 Hz, 2H), 7.75 ppm (d, J=7.4 Hz, 2H); ^{13}C NMR and DEPT (75 MHz, $CDCl_3$): δ=12.07 (CH_3), 12.22 (CH_3), 18.68 (CH_3), 21.21 (CH_2), 22.55 (CH_3), 22.80 (CH_3), 23.84 (CH_2), 24.20 (CH_2), 27.48 (CH_2), 27.92 (3 CH_3), 28.01 (CH_2), 28.23 (CH_2), 28.59 (CH_2), 31.98 (CH_2), 33.96 (CH), 35.46 (C, CH), 35.79 (CH), 36.17 (CH_2), 36.73 (CH_2), 37.18 (CH_2), 39.52 (CH_2), 39.99 (CH_2), 42.60 (C), 44.68 (CH), 47.16 (CH), 50.99 (CH), 54.23 (CH), 56.30 (CH), 56.42 (CH), 67.21 (CH_2), 74.71 (CH), 82.50 (C), 119.96 (2 CH), 125.17 (2 CH), 127.06 (2 CH), 127.69 (2 CH), 141.29 (2 C), 143.81 (C), 143.94 (C), 155.95 (CO), 169.69 (CO), 170.39 ppm (CO); ESI-MS: 782.6 $[M+H]^+$, 799.6 $[M+NH_4]^+$, 804.6 $[M+Na]^+$.

*Fmoc-Asp(ODhc)-OH (**4**)*: TFA (25 mL) was added to a solution of Fmoc-Asp(ODhc)-O*t*Bu (**3a**) (3.72 g, 4.76 mmol) in CH_2Cl_2 (20 mL) and the mixture was stirred for 75 min at room temperature. The mixture was partitioned between water and CH_2Cl_2, and the CH_2Cl_2 layer was washed with water four times. Drying over Na_2SO_4, removal of the solvent, and flash chromatography (petroleum ether/EtOAc [3:2] + 1% HOAc) of the residue on silica gel provided **4** as a colorless solid (2.94 g; 85%). ^{1}H NMR (500 MHz, $CDCl_3$/CD_3OD 8:2): δ=0.67 (s, 3H), 0.80–1.85 (m, 42H), 1.98 (br d, J=12.6 Hz, 1H), 2.87 (dd, J=16.7, 4.8 Hz, 1H), 2.97 (dd, J=16.7, 5.4 Hz, 1H), 4.26 (t, J=7.2 Hz, 1H), 4.38 (m, 2H), 4.60 (t, J=5.1 Hz, 1H), 4.74 (m, 1H), 7.33 (t, J=7.4 Hz, 2H), 7.42 (t, J=7.5 Hz, 2H), 7.63 (t, J=6.8 Hz, 2H), 7.79 ppm (d, J=7.5 Hz, 2H); ^{13}C NMR and DEPT (75 MHz, $CDCl_3$): δ=12.11 (CH_3), 12.25 (CH_3), 18.70 (CH_3), 21.30 (CH_2), 22.57 (CH_3), 22.83 (CH_3), 23.92 (CH_2), 24.28 (CH_2), 27.46 (CH_2); 28.10 (CH), 28.34 (CH_2), 28.68 (CH_2), 32.07 (CH_2), 33.94 (CH_2), 35.55 (CH), 35.57 (C), 35.91 (CH), 36.26 (CH_2), 36.80 (CH_2), 37.08 (CH_2), 39.61 (CH_2), 40.08 (CH_2), 42.69 (C), 44.77 (CH), 47.18 (CH), 50.46 (CH), 54.31 (CH), 56.38 (CH), 56.53 (CH), 67.32 (CH_2), 75.04 (CH), 120.07 (2 CH), 125.24 (2 CH), 127.20 (2 CH), 127.85 (2 CH), 141.39 (2 C), 143.83 (2 C), 156.02 (CO), 170.81 (CO), 172.89 ppm (CO); ESI-MS: 726.5 $[M+H]^+$, 743.5 $[M+NH_4]^+$, 748.5 $[M+Na]^+$. HPLC: ret. time = 48.5 min, 98%; A: H_2O + 0.1% TFA, column: Zorbax Eclipse XDB-C8 (4.6×150 mm, 5 μm), gradient: 10% to 100% B over 45 min; 100% B for 10 min, other conditions as described in the general section.

Synthesis of the fluorophore building block 7:

*Fmoc-Glu(Rho)-OH (**7**)*: EtN*i*Pr$_2$ (1.42 g, 11 mmol, 1.87 mL) was added to a solution of Fmoc-Glu-O*t*Bu (1.56 g, 3.67 mmol), HBTU (1.39 g, 3.67 mmol), and HOBt (562 mg, 3.67 mmol) in DMF (10 mL), and the resulting mixture was stirred for 10 min at room temperature. After addition of a solution of the piperazinyl-modified rhodamine[11] (1.83 g, 3.34 mmol) in DMF (10 mL), the resulting reaction mixture was stirred for 4 h at room temperature. The reaction mixture was poured into water (1 L) and extracted with EtOAc (800 mL). The aqueous layer was saturated with NaCl and extracted once again with ethyl acetate (200 mL). The combined organic layers were washed with brine (2×1 L), dried over Na_2SO_4, and the solvent was removed. Flash chromatography (CH_2Cl_2/MeOH, 10:1) of the crude product on silica gel afforded Fmoc-Glu-(Rho)-O*t*Bu (2.31 g, 72%) as a dark lilac solid. Fmoc-Glu(Rho)-O*t*Bu (2.31 g, 2.42 mmol) was dissolved in a mixture of CH_2Cl_2 (25 mL) and CF_3COOH (5 mL), and the resulting solution was stirred for 2 h at room temperature. The reaction mixture was poured into water (500 mL) and extracted with a mixture of CH_2Cl_2/*i*PrOH, 2:1 (5×300 mL). The combined organic layers were washed with brine and dried over Na_2SO_4. Removal of the solvent and purification of the crude product by flash chromatography on silica gel (CH_2Cl_2/MeOH, gradient elution with 5:1 to 1:1) afforded **7** (2.05 g, 87%) as a dark lilac solid. ^{1}H NMR (500 MHz, CD_3OD): δ=1.34 (br t, J=6.7 Hz, 12H), 1.92–2.03 (m, 1H), 2.22–2.25 (m, 1H), 2.40–2.53 (m, 2H), 3.38–3.46 (m, 8H), 3.72 (br s, 8H), 4.08 (br s, 1H), 4.26–4.28 (m, 1H), 4.36–4.44 (m, 2H), 6.98–7.00 (m, 2H), 7.11–7.20 (m, 2H), 7.28–7.47 (m, 6H), 7.56–7.58 (m, 1H), 7.68–7.74 (m, 3H), 7.82–7.87 ppm (m, 4H); ^{13}C NMR and DEPT (125 MHz, $[CD_3]_2CO$): δ= 12.80 (4 CH_3), 28.13 (2 CH_2), 42.12–42.44 (br, 4 CH_2), 46.50 (4 CH_2), 47.88 (CH), 54.19–54.57 (br, CH), 67.14 (CH_2), 96.80 (2 CH), 114.43 (2 C), 115.08 (3 CH), 117.01 (C), 119.36 (C), 120.70 (2 CH), 126.15 (2 CH), 127.88 (CH), 127.92 (CH), 128.44 (2 CH), 130.52 (CH), 130.66 (CH), 131.24 (CH), 132.06 (C), 132.89 (2 CH), 136.64 (C), 141.92 (C), 144.87 (C), 145.03 (C), 156.51 (C), 157.18 (CO), 158.49 (C), 160.43 (C), 160.70 (C), 167.79 (CO), 171.32 (CO), 173.67 ppm (CO); ESI-MS: *m/z*: 862.5 $[M]^+$, 884.5 $[M-H+Na]^+$.

Solid-phase synthesis of the tripartite compounds 8 and 9:

Typical procedure for the preparation of the fluorophore-labeled peptide:

H-Glu(Rho)-βAla-Gly-Glu-Val-Asn-Sta-Val-Ala-Glu-Phe-4Gl-3Gl-4Gl-3Gl-4Gl-Asp(ODhc)-NH_2 (**8g′**); where Sta is (3*S*,4*S*)-4-amino-3-hydroxy-6-methylheptanoic acid

Loading: Fmoc-Asp(ODhc)-OH (**4**) (363 mg, 0.5 mmol) was dissolved in CH_2Cl_2 (2 mL). HATU (190 mg, 0.5 mmol), DMF (1 mL), and EtN*i*Pr$_2$ (65 mg, 85 μL, 0.5 mmol) were added and the mixture was stirred for 15 min. The resulting clear solution was added to 0.1 mmol of deprotected, low-load (0.21 mmol g^{-1}) PAL-PEG-PS resin. Additional EtN*i*Pr$_2$ (0.5 mmol) and DMF (1 mL) were added. The mixture was stirred slowly for 1 h, transferred to the synthesizer, and subjected to washing, capping, and deprotection.

Automated assembly of 4Gl^{16} to βAla^2: Owing to the high molecular weight, cycles and reaction vessel for the 0.25 mmol scale were used for 0.1 mmol of resin (considerable swelling). Double coupling was used for 4Gl^{16} and coupling times are extended to 50 min.

Coupling of the fluorophore label Glu(Rho)^1: Fmoc-Glu(Rho)-OH (**7**) (293 mg, 0.3 mmol), HATU (114 mg, 0.3 mmol), EtN*i*Pr$_2$ (2×77 mg/2× 102 μL, 2×0.3 mmol), and DMF (4 mL) were used in a procedure similar to the loading step. Automated washing was repeated until the NMP remained colorless.

Cleavage: After washing with CH_2Cl_2 and drying in vacuo, the resin was cleaved with TFA/TIS/anisole/thioanisole/H_2O (87:3:3:3:4; where TIS is triisopropylsilane) at room temperature for 90 min. The resin was removed by filtration and the conjugate was precipitated from the filtrate with Et_2O/hexane (3:7) to afford an oily semisolid, which was collected by centrifugation, taken up in MeCN/MeOH (1:1) and dried in vacuo. Preparative HPLC using H_2O/MeCN/MeOH (85:10:5) + 0.1% TFA as eluent A and a gradient from 40% to 57% of eluent B in 25 min (product: ret. time = 24.1 min) afforded, after drying, **8g′** as a red oil (34 mg; 10%), which slowly solidified in vacuo. HPLC: ret. time = 32.1 min, 98% (gradient from 10% to 100% B over 45 min). ESI-MS: *m/z*: 3346.9 $[M]^+$; (calcd for $^{12}C_{167}{}^{13}C_1H_{270}N_{23}O_{46}{}^+$: M = 3346.9, 100%).

Cell culture: Fertile specific pathogen free chicken eggs (Charles River laboratories) were incubated at 38.5 °C, 55% relative humidity and turned five times a day. Telencephalic cortices were dissected from 8 day-old chicken embryos and cultured according to Pettmann and co-workers.[31] Shortly after removing the meninges, telencephalic hemispheres were digested in a trypsin/EDTA solution (0.05%/0.02%) for 12 min at 37 °C and dissociated by aspiration through a 20-gauge needle. The ho-

mogenate was centrifuged (500 g, 5 min) and resuspended into a medium consisting of Dulbecco's Modification of Eagle's Media (D-MEM) supplemented with 5% fetal calf serum and 5% chicken serum. The cell suspension was passed through a nylon sieve (80 μm) before seeding on polylysine-coated culture plates at a density of 3.75×10^5 cells per cm^2. After 30 min the media was replaced by the cultivation medium (Neurobasal-A-medium, B27 supplements (Invitrogen), 2 mM Glutamin). Cultures were grown at 37°C, 5% CO_2. SH-SY5Y cell lines stably overexpressing APP695 (APPwt) or mutant APP695(KM/NL) (APPsw), both carrying a N-terminal Myc tag and a C-terminal Flag tag[32] were kindly provided by L. Münter and G. Multhaup (Freie Universität Berlin). The cells were cultured in D-MEM/F12, supplemented with 10% fetal calf serum, 2 mM L-glutamine, non-essential amino acids and 50 $\mu g\,mL^{-1}$ Hygromycin B.

Cell viability assays: Cell viability was measured by using the CytoTox 96 lactate dehydrogenase (LDH) assay kit (Promega) and the MTT (3-(4,5-dimethylthiazol-2-yl)-2,5-diphenyltetrazolium bromide) assay.[33]

Inhibitor treatments: The test compounds were initially dissolved in DMSO at a concentration of 10 mM and stored in aliquots at −20°C. For the cell culture experiments, compound dilutions were prepared in 100% DMSO that were added freshly to cell culture medium. The final concentration of DMSO in the experiments and controls was 1%. For CTN cells, the experiments were performed at the 5th day in vitro. The cell culture medium was replaced with fresh medium containing the compounds or 1% DMSO. For each condition four wells of a 24-well plate were used. After an incubation time of 20 h the cell supernatants and cells were collected and pooled. The cells were washed with 2 mM EDTA in PBS and lysed for 10 min on ice with cell lysis buffer (1% Triton X-100 (v/v), 30 mM Tris-HCl, pH 7.4, 150 mM NaCl, 1 mM EDTA, 2 mM DTT, 1x Phospho-Stop (Roche, Mannheim, Germany), 1x complete protease inhibitor cocktail (Roche), 10% Glycerol (v/v)). Cell lysates were obtained in the supernatant after a centrifugation step for 30 min at 16 000 g, 4°C.

For the ECL measurements SH-SY5Y cells were seeded 24 h before treatment in 96-well cell culture plates at a cell density of 1.5×10^5 cells cm^{-2}. The compounds were diluted in the medium and added to the cells as described above. For each condition six wells were used and pooled after an incubation time of 4 h. For Western blot analyses, the cells were seeded into 24-well cell culture plates. Four wells per condition were pooled and the incubation time was prolonged to 24 h. Cell harvesting was performed as described above.

Electrochemiluminescence (ECL) assay: Aβ-peptides in cell supernatants were measured with the MSD Human (6E10) Abeta 40 Kit or the MSD Human (6E10) Abeta 3-Plex 38/40/42 Kit according to the manufacturer's protocol on a Sector Imager 6000 (Meso Scale Discovery). The synthetic reference peptide dilutions were prepared in Neurobasal-A-medium for CTNs or in 1% blocker A for SH-SY5Y cells. The fetal calf serum present in the SH-SY5Y cell culture medium contains bovine Aβ-peptides, which are detected by the ECL assay. The amount of the bovine Aβ40 in unconditioned culture medium was determined to be approximately 50 $pg\,mL^{-1}$, and this background value was subtracted from the calculated Aβ-concentrations in the SH-SY5Y cell culture experiments. Soluble APPα and APPβ were measured with the MSD sAPPα/sAPPβ Multiplex Assay according to the manufacturer's protocol. Synthetic reference peptides were diluted in the cell culture media and were, as well as the samples, supplemented with 50 mM HEPES.

Dose–response curves and EC_{50} determinations: For the calculation of dose–response curves and EC_{50} values for SH-SY5Y APPwt cells, selective compounds were tested in three independent experiments in approximately half-logarithmic serial dilutions ranging from 10 pM to 100 nM. After incubation for 4 h at 37°C and 5% CO_2, the cell culture supernatants from six wells of a 96-well culture plate were pooled and measured in duplicates with the Aβ40 ECL assay. The signals were normalized to percent of the DMSO controls, and the normalized values from the three independent experiments were pooled for calculating dose–response curves and EC_{50} values with GraphPad Prism 5.01 software (GraphPad Software Inc., La Jolla, USA). On SH-SY5Y APPsw cells two different dilution series were tested. In two experiments, the tested concentrations ranged from 10 pM to 100 nM, as described above. To obtain a better definition of the bottom of the curve, in the third experiment, the concentrations were changed to a range from 100 pM to 1 μM. Again, the dose–response curves and EC_{50} values were calculated from the normalized and pooled data from these three independent experiments.

Immunoprecipitation of Aβ-peptides from cell culture supernatants: Magnetic sheep-anti-mouse-IgG Dynabeads M-280 were precoated with the monoclonal antibody 6E10 (Covance, Emeryville, California) (40 $\mu g\,mL^{-1}$) according to the manufacturers protocol (Dynal, Hamburg, Germany). Cell culture supernatants (800 μL) were mixed with 200 μL of a fivefold concentrated IP detergent buffer yielding final concentrations of: 50 mM HEPES, 150 mM NaCl, 0.5% Nonidet P-40 v/v, 0.25% sodium deoxycholate w/v, 0.05% SDS w/v. 25 μL of 6E10-coated magnetic beads were added and immunprecipitation was performed under rotation for 15 h at 4°C. Subsequently, the beads were washed three times for 5 min with PBS/0.1% bovine serum albumin w/v and once for 3 min with 10 mM Tris-HCl, pH 7.5. To elute bound Aβ-peptides, the sample was heated to 95°C for 5 min in 25 μL of sample buffer (0.36 M bis-Tris, 0.16 M Bicine, 1% SDS w/v, 15% sucrose w/v and 0.0075% Bromophenol Blue w/v).

SDS-PAGE, Western blot and immunostaining: The Aβ-peptides were separated on 10% T/5% C polyacrylamide gels by urea-bicine/bis-tris/tris/sulfate SDS-PAGE.[34] For an improved resolution of Aβ-peptides differing at their N-termini, the separation gels were slightly alkalized by reducing the concentration of H_2SO_4 in the separation gel from 0.1 M (original protocol) to 0.075 M without further modifications.

The separated Aβ-peptides were transferred onto Immobilion-P PVDF membranes (Millipore) at 1 $mA\,cm^{-2}$ under semidry conditions (Hoefer Semiphor) for 40 min.[34b] The PVDF-membranes were then boiled for 3 min in hot PBS using a microwave oven to improve antibody binding[35] and blocked afterwards for 1 h at room temperature with 3% milk powder in PBS-T. Immunostaining was performed overnight at 4°C with the antibody 6E10. After washing with PBS-T the membranes were incubated with biotinylated anti-mouse IgG (Linaris, 0.1 $mg\,mL^{-1}$, 45 min, RT), washed again with PBS-T, and finally incubated with a streptavidin horseradish peroxidase complex in PBS-T (GE Healthcare, 1:3000, 45 min, RT).

For the analysis of sAPPα, proteins were separated on 7%T/2.7%C SDS-polyacrylamide gels[36] and blotted afterwards on PVDF membranes by semi-dry transfer for 60 min with 25 mM Tris, 192 mM glycine, 20% (v/v) methanol.[37] Proteins from cell lysates, for analysis of β-CTF, were analyzed by using NuPAGE Novex 4–12% Bis/Tris gels with MES running buffer according to the manufacturer's instructions (Invitrogen). sAPPα and β-CTF blots were blocked for 1 h at room temperature with Rotiblock (Carl Roth GmbH, Karlsruhe, Germany) and probed with monoclonal antibody 1E8 (Bayer Schering Pharma AG, Berlin, Germany) (1:300 dilution). All blots were developed with ECL-plus chemiluminescence according to the manufacturer's instructions (GE Healthcare, Munich, Germany) and detected with an Intas Imager (Intas, Göttingen, Germany). The synthetic peptides were purchased from MoBiTec, Göttingen, Germany.

Two-dimensional SDS-PAGE: Immobilized pH-gradient (IPG) electrofocusing was performed by using dry IPG strips (linear pH range, 7 cm, pH 4–7) on an Ettan IPGphor II IEF System (GE Healthcare). IPG strips were rehydrated in rehydration solution (8.3 M urea, 2% CHAPS w/v, 0.5% Pharmalyte pH 3–10, 20 mM DTT) containing the immunoprecipitated sample, for 10 h at 20°C. Isoelectric focusing was performed as described elsewhere.[25] The separation in the second dimension was performed by urea-SDS-PAGE as described above.

Statistical analysis: Statistical analysis was performed with the GraphPad Prism Software, version 5.01.

Acknowledgements

This work was supported by the European Fund for Regional Development, the State of Saxony (project 4212/06-08), the grant PURE (Protein Research Unit Ruhr within Europe) from the State Government North Rhine-Westphalia, and by the EU grants cNEUPRO (contract no. LSHM-CT-2007-037950) and neuroTAS (contract no. LSHB-CT-2006-037953). We thank H. Kamrowski-Kruck (University of Duisburg-Essen) for excellent technical assistance and L. Münter and G. Multhaup for providing the stably transfected SH-SY5Y cells.

[1] H. Steiner, C. Haass, *Nat. Rev. Mol. Cell Biol.* **2000**, *1*, 217–224.
[2] a) I. Hussain, D. Powell, D. R. Howlett, D. G. Tew, T. D. Meek, C. Chapman, I. S. Gloger, K. E. Murphy, C. D. Southan, D. M. Ryan, T. S. Smith, D. L. Simmons, F. S. Walsh, C. Dingwall, G. Christie, *Mol. Cell. Neurosci.* **1999**, *14*, 419–427; b) X. Lin, G. Koelsch, S. Wu, D. Downs, A. Dashti, J. Tang, *Proc. Natl. Acad. Sci. USA* **2000**, *97*, 1456–1460; c) S. Sinha, J. P. Anderson, R. Barbour, G. S. Basi, R. Caccavello, D. Davis, M. Doan, H. F. Dovey, N. Frigon, J. Hong, K. Jacobson-Croak, N. Jewett, P. Keim, J. Knops, I. Lieberburg, M. Power, H. Tan, G. Tatsuno, J. Tung, D. Schenk, P. Seubert, S. M. Suomensaari, S. Wang, D. Walker, J. Zhao, L. McConlogue, V. John, *Nature* **1999**, *402*, 537–540; d) R. Vassar, B. D. Bennett, S. Babu-Khan, S. Kahn, E. A. Mendiaz, P. Denis, D. B. Teplow, S. Ross, P. Amarante, R. Loeloff, Y. Luo, S. Fisher, J. Fuller, S. Edenson, J. Lile, M. A. Jarosinski, A. L. Biere, E. Curran, T. Burgess, J. C. Louis, F. Collins, J. Treanor, G. Rogers, M. Citron, *Science* **1999**, *286*, 735–741; e) R. Yan, M. J. Bienkowski, M. E. Shuck, H. Miao, M. C. Tory, A. M. Pauley, J. R. Brashier, N. C. Stratman, W. R. Mathews, A. E. Buhl, D. B. Carter, A. G. Tomasselli, L. A. Parodi, R. L. Heinrikson, M. E. Gurney, *Nature* **1999**, *402*, 533–537.
[3] a) B. De Strooper, W. Annaert, *J. Cell Sci.* **2000**, *113*, 1857–1870; b) V. John, J. P. Beck, M. J. Bienkowski, S. Sinha, R. L. Heinrikson, *J. Med. Chem.* **2003**, *46*, 4625–4630.
[4] a) A. Capell, H. Steiner, M. Willem, H. Kaiser, C. Meyer, J. Walter, S. Lammich, G. Multhaup, C. Haass, *J. Biol. Chem.* **2000**, *275*, 30849–30854; b) J. T. Huse, D. S. Pijak, G. J. Leslie, V. M. Lee, R. W. Doms, *J. Biol. Chem.* **2000**, *275*, 33729–33737; c) J. Walter, R. Fluhrer, B. Hartung, M. Willem, C. Kaether, A. Capell, S. Lammich, G. Multhaup, C. Haass, *J. Biol. Chem.* **2001**, *276*, 14634–14641.
[5] a) J. M. Cordy, I. Hussain, C. Dingwall, N. M. Hooper, A. J. Turner, *Proc. Natl. Acad. Sci. USA* **2003**, *100*, 11735–11740; b) R. Ehehalt, P. Keller, C. Haass, C. Thiele, K. Simons, *J. Cell Biol.* **2003**, *160*, 113–123; c) D. R. Riddell, G. Christie, I. Hussain, C. Dingwall, *Curr. Biol.* **2001**, *11*, 1288–1293; d) H. Tun, L. Marlow, I. Pinnix, R. Kinsey, K. Sambamurti, *J. Mol. Neurosci.* **2002**, *19*, 31–35.
[6] a) K. Simons, E. Ikonen, *Nature* **1997**, *387*, 569–572; b) D. A. Brown, E. London, *J. Membr. Biol.* **1998**, *164*, 103–114; c) X. Xu, E. London, *Biochemistry* **2000**, *39*, 843–849; d) D. A. Brown, E. London, *J. Biol. Chem.* **2000**, *275*, 17221–17224; e) K. Simons, D. Toomre, *Nat. Rev. Mol. Cell Biol.* **2000**, *1*, 31–39; f) W. H. Binder, V. Barragan, F. M. Menger, *Angew. Chem.* **2003**, *115*, 5980–6007; *Angew. Chem. Int. Ed.* **2003**, *42*, 5802–5827; g) K. Simons, W. L. C. Vaz, *Annu. Rev. Biophys. Biomol. Struct.* **2004**, *33*, 269–295; h) D. Lingwood, K. Simons, *Science* **2010**, *327*, 46–50.
[7] T. Braxmeier, T. Friedrichson, W. Fröhner, G. Jennings, M. Munick, G. Schlechtingen, C. Schroeder, H.-J. Knölker, K. Simons, M. Zerial, T. Kurzchalia, International Patent, WO 2005/097199, **2005**; PCT/EP2005/003740, **2004**.
[8] a) L. Rajendran, A. Schneider, G. Schlechtingen, S. Weidlich, J. Ries, T. Braxmeier, P. Schwille, J. B. Schulz, C. Schroeder, M. Simons, G. Jennings, H.-J. Knölker, K. Simons, *Science* **2008**, *320*, 520–523; b) R. Martin, J. Kirst, S. Weidlich, H. Schieb, G. Schlechtingen, A. Jäger, L. Rajendran, M. Böhl, S. Richter, R. Fedorov, D. J. Manstein, H. O. Gutzeit, H. Klafki, J. Wiltfang, K. Simons, H.-J. Knölker, *Med. Chem. Res.* **2010**, *20*, S23-S26; c) L. Rajendran, H.-J. Knölker, K. Simons, *Nat. Rev. Drug Discovery* **2010**, *9*, 29–42.
[9] a) M. Citron, T. Oltersdorf, C. Haass, L. McConlogue, A. Y. Hung, P. Seubert, C. Vigo-Pelfrey, I. Lieberburg, D. J. Selkoe, *Nature* **1992**, *360*, 672–674; b) X. D. Cai, T. E. Golde, S. G. Younkin, *Science* **1993**, *259*, 514–516.
[10] J. S. Tung, D. L. Davis, J. P. Anderson, D. E. Walker, S. Mamo, N. Jewett, R. K. Hom, S. Sinha, E. D. Thorsett, V. John, *J. Med. Chem.* **2002**, *45*, 259–262.
[11] A. Capell, L. Meyn, R. Fluhrer, D. B. Teplow, J. Walter, C. Haass, *J. Biol. Chem.* **2002**, *277*, 5637–5643.
[12] a) V. John, International Patent, WO 03/045378, **2003**; PCT/US02/37360, **2002**; b) J. N. Cumming, U. Iserloh, M. E. Kennedy, *Curr. Opin. Drug Discov. Devel.* **2004**, *7*, 536–556.
[13] B. Blankemeyer-Menge, M. Nimtz, R. Frank, *Tetrahedron Lett.* **1990**, *31*, 1701–1704.
[14] T. Nguyen, M. B. Francis, *Org. Lett.* **2003**, *5*, 3245–3248.
[15] L. A. Carpino, H. Imazumi, A. El-Faham, F. J. Ferrer, C. Zhang, Y. Lee, B. M. Foxman, P. Henklein, C. Hanay, C. Mügge, H. Wenschuh, J. Klose, M. Beyermann, M. Bienert, *Angew. Chem.* **2002**, *114*, 457–461; *Angew. Chem. Int. Ed.* **2002**, *41*, 441–445.
[16] R. Wang, J. F. Meschia, R. J. Cotter, S. S. Sisodia, *J. Biol. Chem.* **1991**, *266*, 16960–16964.
[17] L. Hong, G. Koelsch, X. Lin, S. Wu, S. Terzyan, A. K. Ghosh, X. C. Zhang, J. Tang, *Science* **2000**, *290*, 150–153.
[18] D. C. Carrer, S. Weidlich, P. Schwille, H.-J. Knölker, unpublished results.
[19] J. A. Carrodeguas, A. Rodolosse, M. V. Garza, A. Sanz-Clemente, R. Perez-Pe, A. M. Lacosta, L. Dominguez, I. Monleon, R. Sanchez-Diaz, V. Sorribas, M. Sarasa, *Neuroscience* **2005**, *134*, 1285–1300.
[20] M. Citron, D. B. Teplow, D. J. Selkoe, *Neuron* **1995**, *14*, 661–670.
[21] a) H. Yamakawa, S. Yagishita, E. Futai, S. Ishiura, *J. Biol. Chem.* **2010**, *285*, 1634–1642; b) I. Hussain, J. Hawkins, D. Harrison, C. Hille, G. Wayne, L. Cutler, T. Buck, D. Walter, E. Demont, C. Howes, A. Naylor, P. Jeffrey, M. I. Gonzalez, C. Dingwall, A. Michel, S. Redshaw, J. B. Davis, *J. Neurochem.* **2007**, *100*, 802–809.
[22] F. Gruninger-Leitch, D. Schlatter, E. Kung, P. Nelbock, H. Dobeli, *J. Biol. Chem.* **2002**, *277*, 4687–4693.
[23] H. Vanderstichele, M. G. De, N. Andreasen, V. Kostanjevecki, A. Wallin, A. Olsson, K. Blennow, E. Vanmechelen, *Clin. Chem.* **2005**, *51*, 1650–1660.
[24] J. Wiltfang, H. Esselmann, M. Bibl, A. Smirnov, M. Otto, S. Paul, B. Schmidt, H. W. Klafki, M. Maler, T. Dyrks, M. Bienert, M. Beyermann, E. Ruther, J. Kornhuber, *J. Neurochem.* **2002**, *81*, 481–496.
[25] J. M. Maler, H. W. Klafki, S. Paul, S. P. Spitzer, T. W. Groemer, A. W. Henkel, H. Esselmann, P. Lewczuk, J. Kornhuber, J. Wiltfang, *Proteomics* **2007**, *7*, 3815–3820.
[26] a) C. Haass, A. Capell, M. Citron, D. B. Teplow, D. J. Selkoe, *J. Biol. Chem.* **1995**, *270*, 6186–6192; b) R. Cescato, E. Dummermuth, M. Spiess, P. A. Paganetti, *J. Neurochem.* **2003**, *74*, 1131–1139.
[27] a) C. L. Masters, G. Simms, N. A. Weinman, G. Multhaup, B. L. McDonald, K. Beyreuther, *Proc. Natl. Acad. Sci. USA* **1985**, *82*, 4245–4249; b) D. L. Miller, I. A. Papayannopoulos, J. Styles, S. A. Bobin, Y. Y. Lin, K. Biemann, K. Iqbal, *Arch. Biochem. Biophys.* **1993**, *301–307*, 41–52; c) A. E. Roher, J. D. Lowenson, S. Clarke, C. Wolkow, R. Wang, R. J. Cotter, I. M. Reardon, H. A. Zürcher-Neely, R. L. Heinrikson, M. J. Ball, B. D. Greenberg, *J. Biol. Chem.* **1993**, *268*, 3072–3083.
[28] Y. M. Kuo, T. A. Kokjohn, T. G. Beach, L. I. Sue, D. Brune, J. C. Lopez, W. M. Kalback, D. Abramowski, C. Sturchler-Pierrat, M. Staufenbiel, A. E. Roher, *J. Biol. Chem.* **2001**, *276*, 12991–12998.
[29] a) H. Mori, K. Takio, M. Ogawara, D. J. Selkoe, *J. Biol. Chem.* **1992**, *267*, 17082–17086; b) T. C. Saido, T. Iwatsubo, D. M. Mann, H. Shimada, Y. Ihara, S. Kawashima, *Neuron* **1995**, *14*, 457–466.
[30] W. He, C. J. Barrow, *Biochemistry* **1999**, *38*, 10871–10877.
[31] B. Pettmann, J. C. Louis, M. Sensenbrenner, *Nature* **1979**, *281*, 378–380.
[32] L. M. Munter, A. Botev, L. Richter, P. W. Hildebrand, V. Althoff, C. Weise, D. Kaden, G. Multhaup, *J. Biol. Chem.* **2010**, *285*, 21636–21643.
[33] T. Mosmann, *J. Immunol. Methods* **1983**, *65*, 55–63.

[34] a) H. W. Klafki, J. Wiltfang, M. Staufenbiel, *Anal. Biochem.* **1996**, *237*, 24–29; b) J. Wiltfang, A. Smirnov, B. Schnierstein, G. Kelemen, U. Matthies, H. W. Klafki, M. Staufenbiel, G. Huther, E. Ruther, J. Kornhuber, *Electrophoresis* **1997**, *18*, 527–532.

[35] N. Ida, T. Hartmann, J. Pantel, J. Schroder, R. Zerfass, H. Forstl, R. Sandbrink, C. L. Masters, K. Beyreuther, *J. Biol. Chem.* **1996**, *271*, 22908–22914.

[36] U. K. Laemmli, *Nature* **1970**, *227*, 680–685.

[37] H. Towbin, T. Staehelin, J. Gordon, *Proc. Natl. Acad. Sci. USA* **1979**, *76*, 4350–4354.

Received: July 8, 2010
Revised: October 6, 2010
Published online: December 3, 2010

